

## BIOLOGICAL ACTIVITY OF GRAPHENE NANOCOMPOSITES WITH ZINC OXIDE, Cu AND Ag NANOPARTICLES

Boris Martinov<sup>1</sup>, Elitsa Pavlova<sup>2</sup>, Iliana A. Ivanova<sup>3</sup>,  
Lyubomira Yocheva<sup>4</sup>, Anelia Kostadinova<sup>5</sup>, Anna Staneva<sup>1</sup>

<sup>1</sup>University of Chemical Technology and Metallurgy  
8 Kliment Ohridski blvd., 1756 Sofia, Bulgaria

<sup>2</sup>Sofia University „St. Kliment Ohridski“, Faculty of Physics  
5 James Boucher blvd., 1164 Sofia, Bulgaria

<sup>3</sup>Sofia University „St. Kliment Ohridski“, Faculty of Biology  
8 Dragan Tsankov blvd., 1164 Sofia, Bulgaria

<sup>4</sup>Sofia University „St. Kliment Ohridski“, Faculty of Medicine  
1 Koziak Str., 1407 Sofia, Bulgaria

<sup>5</sup>Institute of Biophysics and Biomedical Engineering  
Bulgarian Academy of Sciences, Acad. Georgi Bonchev Str.  
Block 21, 1113 Sofia, Bulgaria  
E-mail: ani\_sta@uctm.edu

Received 18 October 2022  
Accepted 20 December 2022

---

### ABSTRACT

*The aim of this research is to obtain collagen nanocomposites based on graphene, graphene oxide, GO, zinc oxide and metal nanoparticles and to evaluate their pro-, antioxidant and biological activities by luminescent and standard microbiological assays. The antimicrobial activity of graphene composites with added nanosized zinc oxide, silver and copper nanoparticles was tested on Firmicutes bacteria Staphylococcus epidermidis (ATCC 1228) and Gracillicutes Escherichia coli (ATCC 25922). The method of diffusion in agar was used in three variants - spot diffusion, well and paper-disc diffusion. The spot and diffusion disc approaches of the method have shown better effect than the well diffusion for testing the effect of graphene composites on bacteria. The composites with high ZnO content had the best antimicrobial properties against the tested bacteria. The cytotoxicity of the nanocomposites using normal MDCK and A549 epithelial sarcoma cells were tested for 24 h at a concentration of 100 mg mL<sup>-1</sup>. Cancer cells were found to be more sensitive than normal to the graphene composites, proving antitumor activity. The pro- and antioxidant effects of the tested nanomaterials depend on the pH level. At physiological conditions, in the Fenton's system, all but RGO+Cu do not appear to be suitable as an implant nanomaterial. In the H<sub>2</sub>O<sub>2</sub> oxidation system all materials present stable antioxidant effects; only ZnO+RGO+Cu is close to control prooxidant levels. When the nanomaterials are tested for oxidation by O<sub>2</sub><sup>-</sup> radicals, ZnO+RGO and Zn+RGO+Cu show prooxidant effects, as the prooxidant activity is kept for ZnO+RGO even at physiological acidity pH 7.4.*

*Keywords:* nanocomposites, pro- and antioxidant effects, graphene, biological activity, cytotoxicity.

---

### INTRODUCTION

Collagen composites with the participation of graphene and metal nanoparticles have been studied as biomaterials for tissue engineering (especially bone), antibacterial coatings for medical devices (catheters, tubes for medical devices, etc.), porous materials for wound healing, films, etc. They are expected to be biocompatible, with non-toxic degradation products

and opportunities to control their mechanical properties. Collagen is the predominant constituent of all supporting tissues. Its ability to self-organize, biocompatibility and other valuable properties, which can be improved by chemical modification, make it a widely applicable scaffold material for tissue engineering and regenerative medicine. The preparation of similar scaffolds by the cryogenic drying method and the influence of various factors on their physico-chemical, mechanical and

biological characteristics is described in the literature. Collagen can be made into films, sponges and other porous materials for tissue engineering purposes in the creation of skin, peripheral nerve, muscle, cartilage and bone. They are not harmful to living tissue, with non-toxic degradation products and the ability to manage their porosity and mechanical characteristics. An additional advantage of these structural matrices is that the microstructural architecture can be controlled by varying a number of parameters during their fabrication process.

Graphene and graphene nanostructures combine properties that make them an attractive material for both technical and medical applications and the development of composites with their participation enables the creation of new and optimization of existing properties that are important for their applications as multifunctional materials. Their biocompatibility, large specific surface area, and antimicrobial activity are of increasing interest for medical applications, such as cancer diagnosis and treatment, drug delivery, antibacterial and antiviral agents, biosensors, biomaterials for wound healing, and in tissue engineering. In recent years, graphene materials have been highly valued as antibacterial agents due to the resistance of bacteria to multiple agents. Graphene is an allotrope of carbon consisting of a single layer of atoms arranged in two-dimensional honeycomb lattice. There are significant differences in the physico-chemical properties of graphene which is influenced by the production method. Usually, the C atoms at the edges of the particles are not sp<sup>2</sup> hybridised. The edges are stabilised through a number of chemical functionalities including epoxy, hydroxyl and carboxylic groups, the latter giving rise to charge in liquids of high dielectric constant such as water. Thus, the smaller the particles, the higher the ratio of edge groups and therefore charges per unit area. Two-dimensional (2D) materials, like graphene and transition metals, have attracted considerable attention for the last decade due to their unique electrical, optical and mechanical properties [1]. Recently, as their unique characteristics of biocompatibility and biodegradation are known, a lot of publications are focused on applying them in diagnostic, bioabsorbable sensors, and therapeutic applications [2, 3].

A novel Ag/Cu alloy nanoparticles and graphene nanocomposite paste electrode proceed electrochemical

reduction of chlorpyrifos and could be used for detection of environmental pollution [4]. Other biosensor of 3D graphene/copper oxide nano-flowers is intended for detection of organophosphate pesticides [5]. Other 3D graphene sensors were constructed [6]. We have not found many sources related to the study of the biological properties of the graphene nanocomposites presented.

Commonly found bacterium in the digestive tract of animals and humans, *E. coli* is a big challenge for the scientific community in endeavor to preserve the human society from the resistant strains, which cause illnesses in hundreds of thousands of people. In many cases, some strains of *E. coli* could easily exchange genes and plasmids, too. In result, these pathogenic strains have the ability to cause a novel form of disease after adhesion and invasion in the human body due to harmful interference with the other bacteria and gene transfer in the intestine. The representatives of Firmicutes bacteria *Staphylococcus epidermidis* ATCC 12228 and *E. coli* ATCC 25922 are commonly used as a control strains for susceptibility testing to antibiotics and as a quality control strains for commercial products.

Rajapaksha et al. reported about the antibacterial activity of the GO-CuO NPs material investigated using a standard plate count method [7]. The graphene oxide-CuO nanoparticles nanocomposite was determined to be an effective antibacterial nanomaterial, significantly inhibiting the growth of both *E. coli* and *S. typhimurium* bacteria compared to that observed on the pristine GO material. The study suggests that GO-CuO NPs composites are a promising high-efficacy antibacterial nanomaterial.

The aim of our study is to compare the biological effect of some graphene composites on both Gracilicutes and Firmicutes bacteria, tumor and cancer cell lines as well as their prooxidant and antioxidant activities. The free radical reactions and formation of reactive oxygen species are vital metabolic responses that ensure body's homeostasis, functional activity and adaptation. The speed of these reactions is maintained by a complex system of regulation, and its imbalance is a universal mechanism and cause for the development of chronic and acute bacterial and viral infections, atherosclerosis, cardiac, nephrological and neurodegenerative diseases, etc. Today, such a mechanism of cellular damage has been established for over 100 diseases with different etiologies [8].

## EXPERIMENTAL

### Preparing of nanocomposites

Six composites based on nanosized zinc oxide, copper and silver and graphene materials were prepared for the experiment. Samples 1 and 2 are based on zinc oxide and 5 mass % RGO (95 mass % ZnO x 5 mass % RGO), as in number two (95 mass % ZnO x 5 mass %) (RGO + 5 mass % Cu). Sample number 3 contains 75 mass % RGO and 25 mass % Cu ( $\text{Cu}^0$ ,  $\text{Cu}_2\text{O}$ ). Sample number 4 contains 75 mass % RGO and 25 mass % Ag. Sample number 5 contains 80 mass % GO and 20 mass % ZnO, Sample number 6 contains 88 mass % RGO and 12 mass % Cu NPs.

In order to test the antibacterial properties, the selected graphene materials were synthesized (Table 1). The initial components - GO, nanosized ZnO and Cu nanoparticles, necessary for the synthesis of the composites were synthesized earlier [9, 10]. The obtained starting materials were characterized by X-ray diffraction, SEM and EDX analysis and the production of monophasic products was demonstrated.

The starting components were weighed in ratios presented in Table 1, mixed and homogenized in an agate mill. Distilled water was added to the desired concentration of nanoparticles and the resulting suspension was sonicated in an ultrasonic reactor for one hour (Fig. 1). In addition to the obtained water solutions of the presented composites, collagen solutions of the same were also prepared. For this purpose, enzymatically fragmented collagen is added to obtain a 1 % concentration and the resulting suspension is subjected to stirring on a magnetic stirrer and to ultrasonic treatment using an ultrasonic reactor for 30 min. Using the ultrasonic treatment, a very good distribution of nano-sized ZnO, Ag and Cu on the graphene layers is achieved, which is proven using TEM analysis [9]. Fibrillar collagen „Type I“ gel with a concentration of 60 wt. % was used for the synthesis of the collagen composites. The concentration of the collagen gel was adjusted to 1 % and the pH to 7 using 1M sodium hydroxide (NaOH) solution. The appropriate antimicrobial agent is added to it.

The obtained collagen suspensions were subjected to antibacterial tests against bacteria *Escherichia coli* ATCC 25922 and *Staphylococcus epidermidis* ATCC 1228. Five dispersions in saline (0.9 mass % NaCl)

at a concentration of 1 mg mL<sup>-1</sup> were prepared. The dispersions were sonicated in a Bandelin RK31 bath for two consecutive days for one hour. For the treating of microorganisms, dispersions were prepared in the ratios 1: 1, 1: 4, 1: 9 with sterile saline solution.

### Microorganisms

The antimicrobial effect was tested on representatives of Gram-positive and Gram-negative bacteria: a strain of *Staphylococcus epidermidis* ATCC 1228 and *Escherichia coli* ATCC 25922, supplemented from the National Bank of Industrial microorganisms and cell cultures (NBIMCC), Bulgaria. They were cultured in a nutrient broth (NB Conda, Spain) at 37°C and 180 rpm (shaker Rotomax, incubator Binder, Germany), and sub-cultivated every 12 hours to reach the exponential phase. The optical density of the inoculum in exponential phase was 0.5 for *Escherichia coli* ATCC 25922 and 0.7 for *Staphylococcus epidermidis* ATCC 1228 determined according to McFarland and used for the experiments.

### Antimicrobial activity

The spot diffusion test in agar medium was used to investigate the antibacterial effect of the nanoparticles.

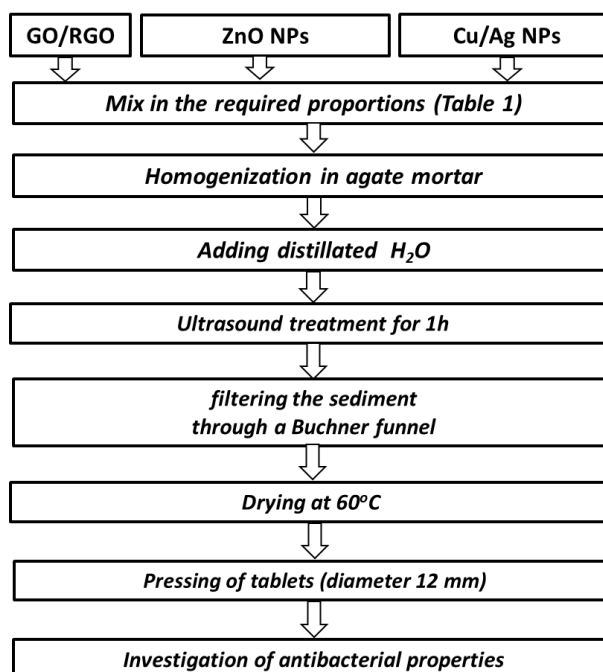


Fig. 1. Scheme for the synthesis of collagen suspensions on graphene composites.

The aliquots of 100  $\mu\text{L}$  microbial suspension in exponential phase with optical density mentioned above were randomly spread on solid medium (Nutrient agar, Conda, Spain) and 10  $\mu\text{L}$  drops of the dispersions with concentrations: 1  $\text{mg mL}^{-1}$ ; 0.5  $\text{mg mL}^{-1}$ ; 0.33  $\text{mg mL}^{-1}$ , and 0.1  $\text{mg mL}^{-1}$  of the investigated material, were put on them. The plates were left for 20 h at 4°C to afford diffusion of the dispersions and after that incubated at 37°C for 24 h. The formed sterile zones around the droplets samples were measured in mm ( $\pm 0.5$ ) as a preliminary fast screening.

The diffusion in agar wells was also used. *E. coli* ATCC 25922, and *Staphylococcus epidermidis* ATCC 1228 suspensions in exponential phase were inoculated in melted and cooled till 44°C - 46°C nutrient agar and randomly distributed in Petri dishes in quantity 20 mL. Solidified medium wells with 8 mm diameter are punched aseptically with a sterile cork borer and 30 mL suspension of the newly synthesized graphene nanocomposites were dropped. The plates were left in refrigerator for 2 h and after that incubated as mentioned above [11].

The paper disc diffusion test was the third method used to assess the antimicrobial effect. *E. coli* ATCC 25922 and *Staphylococcus epidermidis* ATCC 1228 suspensions in exponential phase were inoculated in melted and cooled till 44°C - 46°C nutrient agar and randomly distributed in Petri dishes in quantity 20 mL. Paper discs soaked with 20  $\mu\text{L}$  of different nanoparticles suspensions were placed on solidified medium after drying 24 h. The formed sterile zones around the droplets samples were measured in mm ( $\pm 0.5$ ) and photographed.

### Cell lines

Cytotoxicity was evaluated against 2 types of eukaryotic cells: model MDCK II kidney epithelial cell line and A549 lung alveolar sarcoma cell line all provided from the NBIMCC, Bulgaria. The used eukaryotic cells were maintained at standard conditions in humidified atmosphere with 5 %  $\text{CO}_2$ , at 37°C, in the corresponding medium DMEM (SIGMA), supplemented with 10 % FBS (BioWhittaker TM) and 1 % (v/v) antibiotic-antimycotic solution (penicillin 100 U/mL, streptomycin 100  $\mu\text{g mL}^{-1}$  and amphotericin B 0.25  $\mu\text{g mL}^{-1}$ , BioWhittaker TM). After 24 hours, the cytotoxicity was evaluated by crystal violet test and the cell morphology was observed by bright field microscopy.

### Crystal violet staining and microscopic observation

Crystal violet staining was performed with some modifications [12]. The values of optical density were read on a micro plate reader (TECAN Spectrometer, Germany) at 570 nm wavelength and the number of vital cells was calculated as a percentage from their total amount. Invert microscope pictures were taken out using supplied with a digital camera DV-130, XDS-2A microscope, China.

### Cytotoxicity tests

The crystal violet staining was performed as follows: the residual cell monolayer was washed with phosphate-buffered saline (PBS) and fixed with 4 % PFA in PBS. After that, plates were washed with water and 200  $\mu\text{L}$  of 1 % crystal violet solutions was added to every well. After 20 min of incubation at room temperature, plates were washed with water and processed as described above.

### Chemiluminescent assay

The effect of nanomaterials on the kinetics of free-radical oxidation reactions in ex vivo buffer systems is investigated under different reaction conditions - physiological pH 7.4 and pH 8.5 (acidity of the medium favoring radical formation reactions, meaning that better differential comparison between the measured signals can be recorded). We have applied the following model systems, using activated chemiluminescence and the probe lucigenin:

- 1) Chemical, with Fenton's reagent ( $\text{H}_2\text{O}_2$ - $\text{FeSO}_4$ ) - for the generation of hydroxyl radicals ( $\text{OH}\cdot$ );
- 2) Chemical, with oxidant hydrogen peroxide ( $\text{H}_2\text{O}_2$ );
- 3) Chemical (NAD.H-PhMS), for the generation of superoxide radicals ( $\text{O}_2^{\cdot-}$ ).

The control systems contain the same reagents and final concentrations as the tested samples, without nanomaterials. The reactions are monitored for a period of 3 minutes every 3 seconds; the peak for the curve obtained (maximum value) is determined. In the chemiluminescent assay, only 1  $\text{mg mL}^{-1}$  concentration of the nanomaterials is applied.

### Statistics

All results were obtained as triplicate reproducible measurements, statistically processed by Origin 8.5 and Microsoft Office Excel 2010.

## RESULTS AND DISCUSSION

### Antibacterial effect of graphene nanocomposites

Various dispersions composed of graphene oxide obtained by the Hammer method and with added metal nanoparticles prepared and sonicated as described in the Materials and Methods section were investigated. It was used graphene concentration, four dilutions for each of the six solutions - 5.0; 2.5; 1.0 and 0.5 mg mL<sup>-1</sup> were prepared with and without collagen and were measured the sterile areas (Table 1).

It should be noted that the results of this experiment have shown similar toxicity against both bacteria *E. coli* and *S. epidermidis*, with different cell-wall structure. Gram-positive bacteria are usually more sensitive and show larger sterile areas [13, 14]. In this case, the dispersions of nanocomposites were prepared with

collagen, which may improve the toxicity effect of the nanocomposites.

The largest sterile zone is obtained in the nanocomposite of reduced graphene oxide with zinc oxide and copper, almost the same as with the composite RGO:ZnO. Both composites have a significantly stronger antibacterial effect than the composite with reduced graphene oxide and silver nanoparticles. This is probably due to the high mass concentration of zinc oxide nanoparticles, which are known to have the ability to generate oxygen free radicals upon contact with microbial cells. The composite of reduced graphene oxide and copper nanoparticles has the lowest measured sterile zone, probably due to the fact that copper ions are important cofactors in a number of cellular enzymes and have a toxic effect only in high concentrations [15, 16]. When the nanocomposites contain approximately

Table 1. Antimicrobial effect on paper disks impregnated with 20 µL graphene composites.

No	Nanocomposite	Dilution (in sterile saline)	<i>E. coli</i> ATCC 25922 (inhibitory zone, ± 0.5 mm) (Disc - 5 mm) 20 mL	<i>S. epidermidis</i> ATCC 1228 (inhibitory zone, ± 0.5 mm) (Disc - 5 mm) 20 mL
1.	95 mass % ZnO x 5 mass % RGO (ZnO/RGO)	5 mg mL <sup>-1</sup>	15	9
		1:1	12	8
		1:4	8	8
		1:9	7	7
2.	95 mass % ZnO x 5 mass % (RGO+5 mass % Cu) ZnO/RGO Cu	5 mg mL <sup>-1</sup>	13	10
		1:1	12	8
		1:4	10	8
		1:9	9	7
3.	75 mass % RGO / 25 mass % Cu(Cu <sup>0</sup> , Cu <sub>2</sub> O) (RGO/Cu, Cu <sub>2</sub> O)	5 mg mL <sup>-1</sup>	8	9.5
		1:1	7	8.5
		1:4	6	8
		1:9	5	7
4.	75 mass % RGO /25 mass % Ag (RGO/Ag)	5 mg mL <sup>-1</sup>	10	7
		1:1	8	6
		1:4	8	6
		1:9	7	6
5.	80 mass% GO /20 mass % ZnO (GO/ZnO)	5 mg mL <sup>-1</sup>	9	9
		1:1	8	7
		1:4	6	6
		1:9	5	6
6.	88 mass % RGO + 12 mass % Cu (RGO/Cu (12 %))	5 mg mL <sup>-1</sup>	6	5
		1:1	6	5
		1:4	5	5
		1:9	5	5



Table 2. Antimicrobial effect on 30  $\mu$ L graphene composites suspensions and collagen/graphene nanocomposites in wells.

No	Nanocomposite	Dilution (in sterile saline)	<i>E. coli</i> ATCC 25922 (inhibitory zone, $\pm$ 0.5 mm) (well - 8 mm) 30 mL	<i>S. epidermidis</i> ATCC (inhibitory zone, $\pm$ 0.5 mm) (well - 8 mm) 30 mL	1% collagen solution	<i>E. coli</i> ATCC 25922 (inhibitory zone, $\pm$ 0.5 mm) (well - 8 mm) 30 mL	<i>S. epidermidis</i> ATCC 1228(inhibitory zone, $\pm$ 0.5 mm) (well - 8 mm) 30 mL
1.	95 mass% ZnO x 5 mass% RGO (ZnO/RGO)	5 mg mL <sup>-1</sup> 1:1 1:4 1:9	10.5 10 8 8	8 8 8 8	5 mg mL <sup>-1</sup> 1:1 1:4 1:9	18.5 17 8 8	15 13 - -
2.	95 mass% ZnO x 5 mass% (RGO+5 mass% Cu) ZnO/RGO Cu	5 mg mL <sup>-1</sup> 1:1 1:4 1:9	10.5 8 8 8	8 8 8 8	5 mg mL <sup>-1</sup> 1:1 1:4 1:9	18 11 8 8	14 13 8 8
3.	75 mass% RGO / 25 mass% Cu(Cu <sup>0</sup> , Cu <sub>2</sub> O) (RGO/Cu, Cu <sub>2</sub> O)	5 mg mL <sup>-1</sup> 1:1 1:4 1:9	8 8 8 8	8 8 8 8	5 mg mL <sup>-1</sup> 1:1 1:4 1:9	15 8 8 8	10 9 8 8
4.	75mass% RGO /25 mass% Ag (RGO/Ag)	5 mg mL <sup>-1</sup> 1:1 1:4 1:9	8 8 8 8	9 8 8 8	5 mg mL <sup>-1</sup> 1:1 1:4 1:9	11 8 8 8	11 10 9 8
5.	80 mass % GO /20 mass % ZnO (GO/ZnO)	5 mg mL <sup>-1</sup> 1:1 1:4 1:9	15 8 8 8	15 8 8 8	5 mg mL <sup>-1</sup> 1:1 1:4 1:9	19 14 8 8	16 11 8 8
6.	88 mass % RGO + 12 mass % Cu (RGO/Cu (12 %))	5 mg mL <sup>-1</sup> 1:1 1:4 1:9	8 8 8 8	8 8 8 8	5 mg mL <sup>-1</sup> 1:1 1:4 1:9	8 8 8 8	8 8 8 8

Table 3. Antimicrobial effect on paper disks soaked with certain quantity of antibiotics in  $\mu\text{g}$ .

Antibiotic	Concentration in mg of antibiotic (5 mm disc)	<i>E. coli</i> ATCC 25922 (Inhibition zone)	<i>S. epidermidis</i> ATCC (Inhibition zone)
Rifampicin	5 mg/disc	17 mm	10 mm
Cephalotin	30 mg/disc	5 mm	5 mm
Fosfomycin	200 mg/disc	15 mm	5 mm
Imipenem	25 mg/disc	15 mm	5 mm

the same amount of silver or nanosized zinc oxide nanoparticles, then the results show a stronger antimicrobial effect of the composite containing silver nanoparticles. At the same mass percentages of silver and copper nanoparticles, silver has a stronger effect too.

The results of these experiments show a strong concentration dependence on the content of metal nanoparticles for the antibacterial activity of the nanocomposites. We can arrange the toxicity of the metal nanoparticles inlaid on graphene layers as follows:  $\text{Ag} > \text{ZnO} > \text{Cu}$ . The tested antibiotics give similar sterile zones (Table 3). It is important to mention that collagen suspensions of all tested nanoparticles have stronger effect on both bacteria in concentrations 5 and 2.5 mg  $\text{mL}^{-1}$  no matter if they are placed in agar wells or using paper disks. The results could be explained with better dispersability of nanoparticles on collagen proteins and better interaction with bacteria. It could be suggested, that collagen prevents the agglomeration of nanoparticles and improves their interaction with both bacteria.

### Cell viability and antitumor effect of graphene nanocomposites

To assess the cytotoxicity of the nanocomposites on different cell lines, crystal violet and spectrophotometric reading of the cell survival were used (Fig. 2). The cells from the MDCKII kidney epithelial line and lung sarcoma cells from the A549 line were incubated for 24 h with graphene nanocomposites in concentrations of 100  $\mu\text{g mL}^{-1}$ .

After photometric reading of the results, we found that on material ZnO/RGO, ZnO/RGO Cu, and RGO/ZnO, the survival of the cells was very low (5 % - 8 %), while on materials, RGO/Cu,  $\text{Cu}_2\text{O}$ , RGO/Ag, GO/ZnO there was a higher survival of about 50 % - 60 % in MDCK and 20 % - 30 % in tumor A549 cells, as

these values are only in the lowest concentration of the nanocomposites (Fig. 3). Material ZnO/RGO was also low in cytotoxicity for both cell line types. The morphological data also supported the cell survival results; in materials ZnO/RGO and ZnO/RGO Cu the cells were completely rounded and most of them were in cell suspension, in materials RGO/Cu,  $\text{Cu}_2\text{O}$ , RGO/Ag, GO/ZnO, RGO/ZnO there were also rounded cells, but there more than 50 % were well spread with a typical polygon shape, again having more dead cells in the A549 cell line. From our cytotoxicity and cell morphology studies, it can be concluded that the graphene nanocomposites in high concentrations are as toxic as normal and at low concentrations, only materials ZnO/RGO, ZnO/RGO Cu and RGO/ZnO are toxic to both cell lines, while at low concentrations of graphene composites, graphene nanocomposites RGO/Cu,  $\text{Cu}_2\text{O}$ , RGO/Ag, GO/ZnO, RGO/ZnO have good cell survival in MDCK cells, which is a model of noncancerous cells, while lung sarcoma A 549 ones have low survival. We can conclude that to material, RGO/Cu,  $\text{Cu}_2\text{O}$ , RGO/Ag, GO/ZnO, RGO/ZnO the cells have a specific response, as the cancer cells have many lower survival than the model of non-cancerous cells -MDCK cell line. We can conclude that materials RGO/Cu,  $\text{Cu}_2\text{O}$ , RGO/Ag, GO/ZnO, RGO/ZnO have anticancer activity by maintaining cell survival in normal cells and killing cancer cells.

The chemiluminescent method allows tracing of the concentration and kinetics of free radical formation with small amounts of sample. It is easy to determine the quantum yield of these reactions (480 nm - 580 nm). This is a suitable, reliable, highly sensitive, express and relatively inexpensive method for in vitro/ex vivo testing. This method allows to monitor the dynamics of free radical reactions and to determine their prooxidant/antioxidant activity. The spontaneous, metabolic

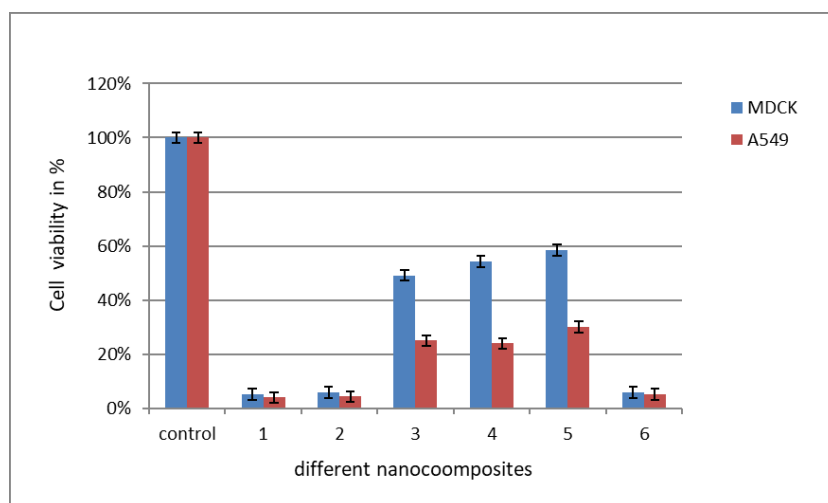


Fig. 2. Cell viability in polystyrene plaques of kidney epithelial cells (MDCK) and lung sarcoma A549 cells. Control, 1 - ZnO/RGO, 2 - ZnO/RGO Cu, 3 - RGO/Cu, Cu<sub>2</sub>O, 4 - RGO/Ag, 5 - GO/ZnO, 6 - RGO/Cu (12 %).

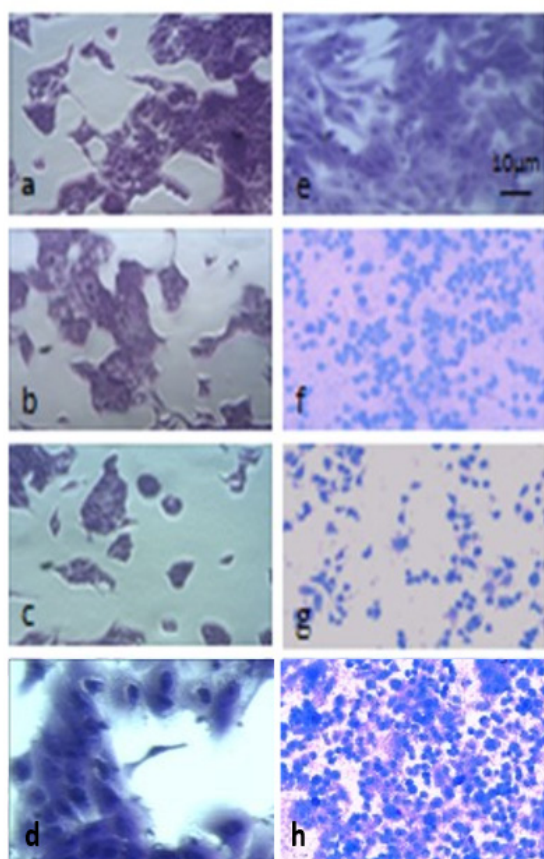


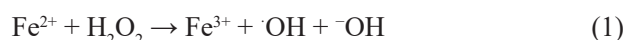
Fig. 3. Cell morphology in polystyrene well plate of kidney epithelial (MDCKII) (a), ZnO/RGO (b) ZnO/RGO Cu, (c) RGO/Ag, (d) GO/ZnO and lung sarcoma A549 cells (e) RGO/ZnO, (f) ZnO/RGO Cu, (g) RGO/Ag, (h) GO/ZnO (Magnification 200x).

chemiluminescence can be enhanced by physical and chemical activators (probes), such as luminol, lucigenin and many other specific or nonspecific traps of hydroxyl and/or superoxide anion radicals and other reactive oxygen species as the reaction is accompanied with light emission. The automatic computer processing in these studies allows to register the kinetics of the reaction and to determine the values of the rate constants and other parameters when interacting with the test substances [17 - 21].

In the following selected chemiluminescent model systems, the given concentrations are final, with total volume of 2 mL; the lucigenin probe is dissolved in dimethyl sulphoxide as a final volume of 20  $\mu$ L in order not to suppress the signal:

#### • System 1

The sample contains 0.2 mol sodium hydrogen phosphate buffer, with the appropriate pH, Fenton's reagent: FeSO<sub>4</sub> ( $5 \cdot 10^{-4}$  mol) - H<sub>2</sub>O<sub>2</sub> (1.5 %), lucigenin ( $10^{-4}$  mol) and nanomaterials. It is well known that the interaction between Fe<sup>2+</sup> ions and H<sub>2</sub>O<sub>2</sub> results in the generation of highly reactive, short-living  $\cdot$ OH and  $\cdot$ OOH radicals. The chemiluminescent emission from this reaction is much higher than from other mixtures:





At pH 8.5 all nanomaterials except RGO+Ag and GO+ZnO exhibit prooxidant effects compared to the control (Fig. 4(A)). The increase in the signal is as follows: ZnO+RGO – 2.25 times higher, ZnO+RGO+Cu - 1.62 times higher, RGO+Cu<sup>0</sup> and RGO+Cu - approximately to control levels. RGO+Ag and GO+ZnO have antioxidant properties presented as 20 % inhibition of the signal. The kinetics is with constant levels, no fast flashes, peaks or minimums are registered. This is due to the profound properties of the nanomaterials as pro- or antioxidants. That effect can be probably followed for a long period of time.

At pH 7.4 the oxidation process registered by chemiluminescence is inhibited by all nanomaterials but RGO + Cu (Fig. 4(B)). All the other materials show

profound antioxidant effect against the generated ROS such as  $\cdot\text{OH}$  and  $\cdot\text{OOH}$  radicals, registered as 10 % -30 % inhibition of the signal. Most effective is GO+ZnO. The prooxidant activity of RGO+Cu is only about 10 %. It should be noticed that at pH 8.5 most materials present prooxidant activity which is converted into antioxidant at lower acidity. In fact, pH 7.4 is almost neutral and corresponding to the physiological pH within the organism. But in both cases RGO+Cu does not appear to be suitable as an implant nanomaterial.

### • System 2

The sample contains 0.2 mol sodium hydrogen phosphate buffer, with appropriate pH,  $\text{H}_2\text{O}_2$  (1.5 %), the chemiluminescent probe lucigenin ( $10^{-4}$  mol) and

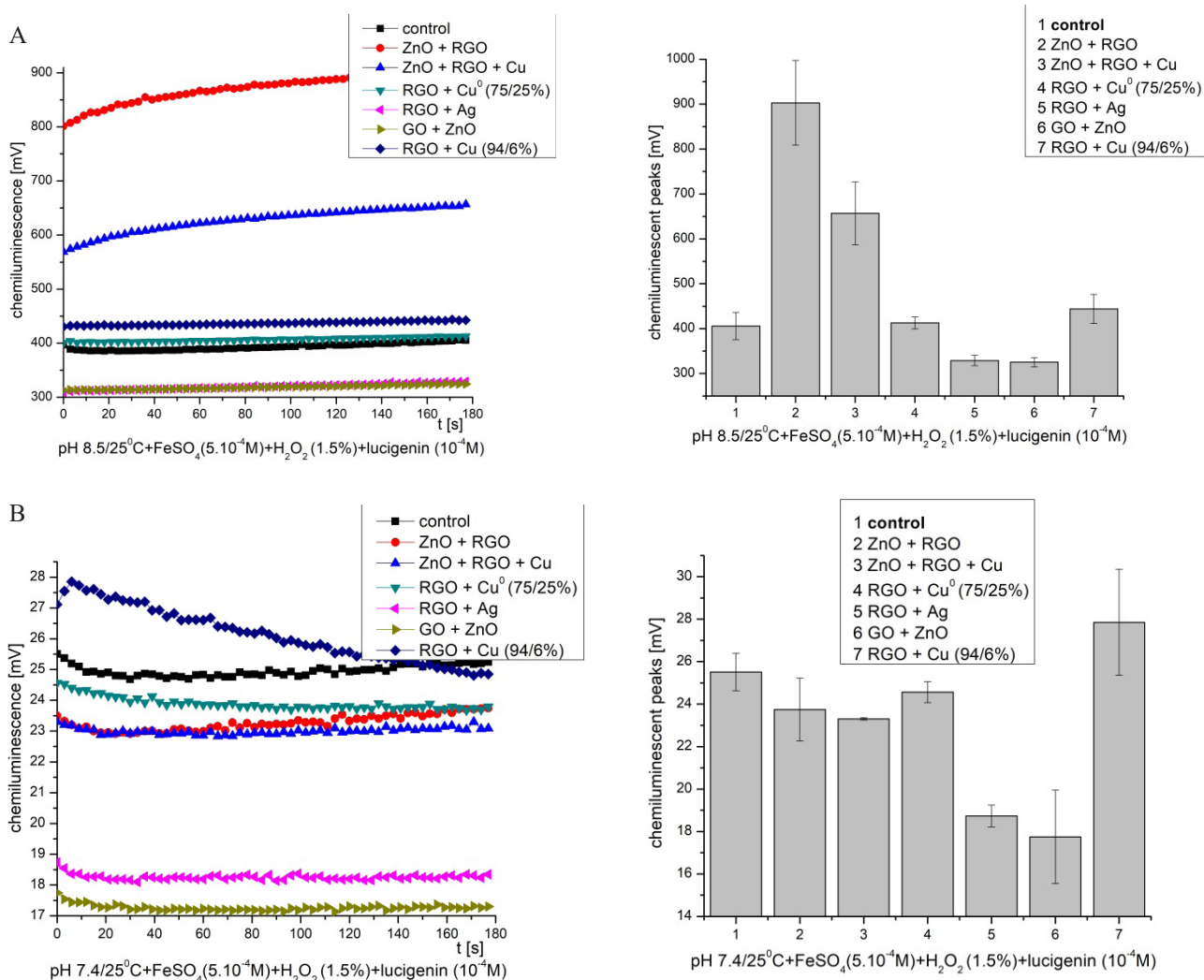


Fig. 4. Chemiluminescence induced by  $\cdot\text{OH}$  and  $\cdot\text{OOH}$  radicals at pH 8.5 (A) and pH 7.4 (B) and the effect of nanomaterials (the data are presented as means  $\pm$  SEM of 3 independent experiments,  $p \leq 0.05$ ).

nanomaterials. In this system, hydrogen peroxide plays both the role of an oxidizing agent and a reactive oxygen species.

All tested nanomaterials exhibit pronounced antioxidant activity against  $\text{H}_2\text{O}_2$  at pH 8.5 (Fig. 5(A)). Despite huge standard deviations all materials present stable antioxidant effect between 10 % and 25 % that is prolonged with time. Most effective is RGO+Cu (94/6 %) . The kinetics is flat, without fast flash maximums and lower minimal areas. This is to confirm the profound activity of nanomaterials also shown in system 1.

The antioxidant activity towards  $\text{H}_2\text{O}_2$  is also kept at physiological pH 7.4 (Fig. 5(B)). Huge standard deviations about some of the materials are also observed, describing them as unstable towards the oxidation from

$\text{H}_2\text{O}_2$ . The kinetics is flat with minor deviations, with no definite maximums or minimums. The antioxidant effect compared to controls varies from 2 % to 22 %. Most effective is RGO+Ag. Only ZnO+RGO+Cu is close to control levels.

### • System 3

The sample contains 0.2 mol sodium hydrogen phosphate buffer, with the corresponding pH, NAD.H ( $10^{-4}$  mol), phenazine-metasulfate ( $10^{-6}$  mol), lucigenin ( $10^{-4}$  mol) and nanomaterials. The scheme for the generation of superoxide radicals in this chemical system is the following [22, 23].

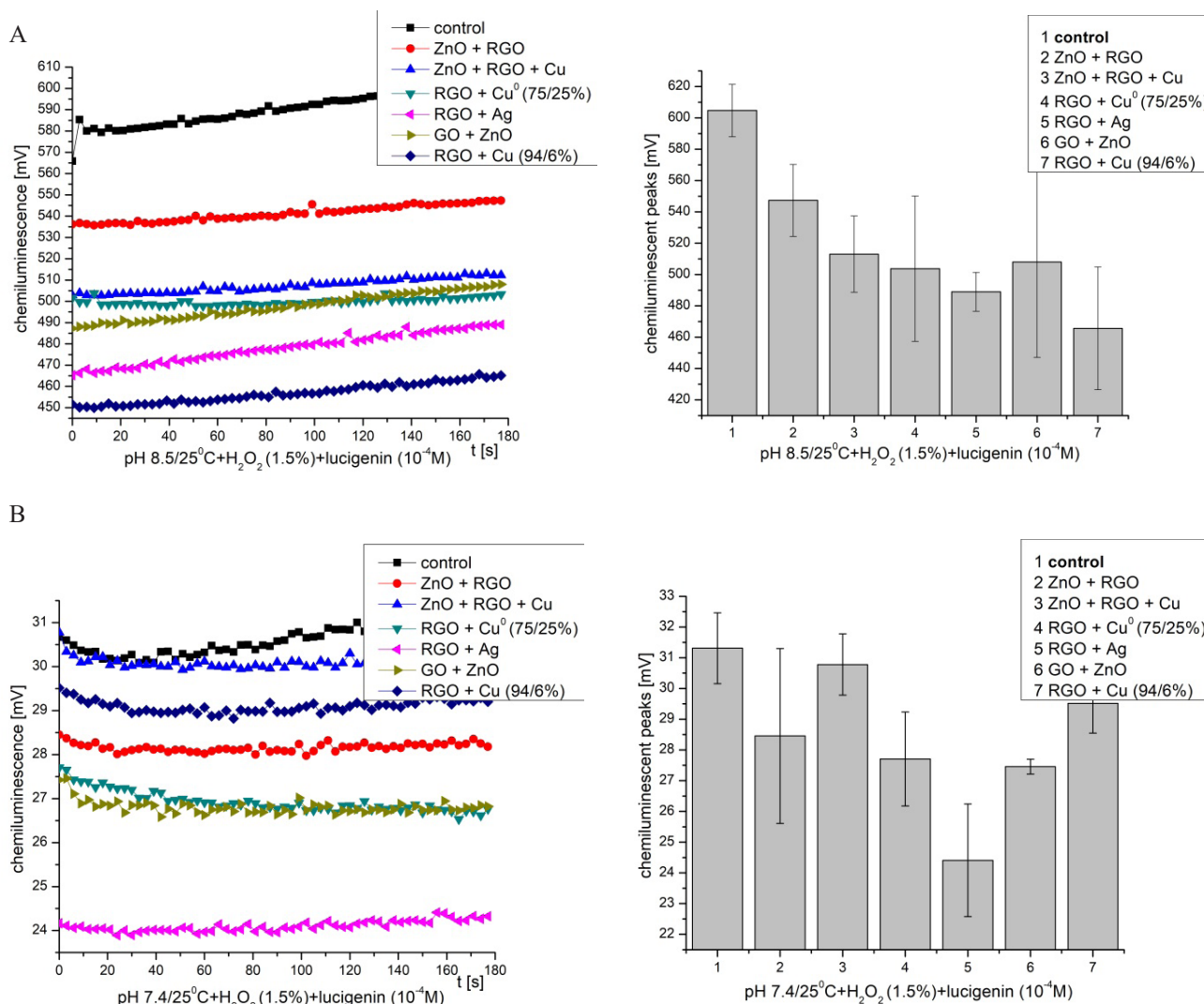


Fig. 5. Chemiluminescence induced by  $\text{H}_2\text{O}_2$  at pH 8.5 (A) and pH 7.4 (B) and the effect of nanomaterials (The data are presented as means  $\pm$  SEM of 3 independent experiments,  $p \leq 0.05$ ).

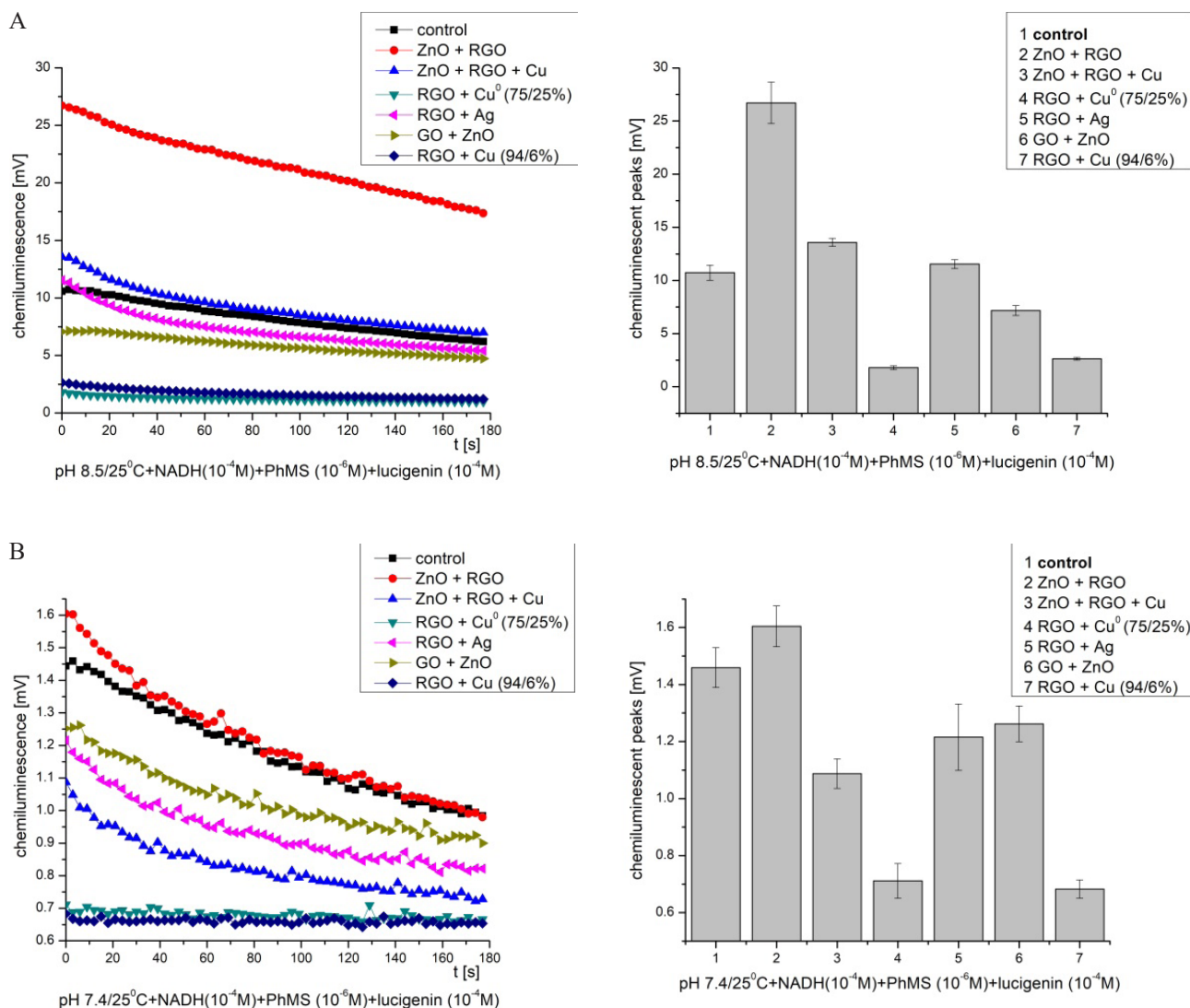
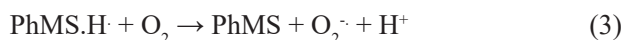


Fig. 6. Chemiluminescence induced by  $O_2^{\cdot-}$  radicals at pH 8.5 (A) and pH 7.4 (B) and the effect of nanomaterials (the data are presented as means  $\pm$  SEM of 3 independent experiments,  $p \leq 0.05$ ).



At pH 8.5 ZnO+RGO exhibits strong prooxidant properties (2.5 times higher than the control), followed by Zn+RGO+Cu which is oxidized close to control levels (Fig. 6(A)). The other tested nanomaterials present antioxidant properties starting from 30% activity as most effective is RGO+Cu (about 80 %). All materials are stable towards the oxidation by the superoxide radicals that are generated in this model system.

When the nanomaterials are tested for oxidation by  $O_2^{\cdot-}$  radicals at pH 7.4 it is observed a characteristic fast flash in the beginning of the reaction for 20 sec followed by slow decrease of the signal (Fig. 6(B)). Such kinetics is not observed for none of the other tested

model systems. Only ZnO+RGO shows prooxidant activity but very close to the control oxidation level. All the other nanomaterials present as antioxidants with various effectivity. Soft to mild properties are exhibited by GO+ZnO, RGO+Ag and ZnO+RGO+Cu (15 % to 25 %); RGO+Cu present strong antioxidant activity, about 50 % inhibition in comparison to the control.

## CONCLUSIONS

The results of antimicrobial experiments with *E. coli* and *S. epidermidis* show a strong concentration dependence on the content of metal nanoparticles for the antibacterial activity of graphene nanocomposites.

We can arrange the toxicity of metal nanoparticles inlaid on graphene layers as follows: Ag > ZnO > Cu. The tested control antibiotics give similar sterile zones. The combination of nanoparticles and antibiotics will have synergistic effect on bacteria. The spot-diffusion and well diffusion tests give better results than the disk diffusion method. The last results mean that paper prevents diffusion of nanoparticles and their interaction with bacteria. Collagen suspensions of all tested nanoparticles have stronger effect on both bacteria in concentrations 5 and 2.5 mg mL<sup>-1</sup> than nanoparticle suspensions without collagen.

At pH 8.5 in the Fenton's system all nanomaterials except RGO+Ag and GO+ZnO (20 % inhibition) exhibit prooxidant effects compared to the control. This activity is converted into antioxidant at lower acidity (pH 7.4). However, in both cases, RGO+Cu does not appear to be suitable as an implant nanomaterial.

When H<sub>2</sub>O<sub>2</sub> is applied as an oxidant at pH 8.5 all materials present stable antioxidant effect between 10 % and 25 %. It is also kept at physiological pH 7.4. Only ZnO+RGO+Cu is close to the control level.

When the nanomaterials are tested for oxidation by O<sup>2-</sup> radicals at pH 8.5, ZnO+RGO are oxidized 2,5 times higher than the control, followed by Zn+RGO+Cu - close to the control level. The other nanomaterials present antioxidant properties starting from 30 % activity as the most effective is RGO+Cu (about 80 %). At pH 7.4 only ZnO+RGO shows light prooxidant activity. All the others present as antioxidants with various effectivity (15 % - 50 %).

The pro- and antioxidant effect of the tested nanomaterials depends on the pH level. This should be considered in their applications.

Our investigations for the cell cytotoxicity showed that the nanocomposites RGO/Cu, Cu<sub>2</sub>O, RGO/Ag, GO/ZnO, RGO/ZnO have anticancer activity by maintaining the cell survival in normal cells and killing the cancerous cells.

### Acknowledgements

*Authors acknowledge the financial support of the National Science Fund of Bulgaria, Project KII-06-H27/17 17.12.2018 and Project "Clean technologies for sustainable environment - waters, waste, energy for circular economy", Ministry of*

*Education and Science, Bulgaria, Contract Number: BG05M2OP001-1.002-0019.*

### REFERENCES

1. S.M. Notley, R.J. Crawford, E.P. Ivanova, Bacterial interaction with graphene particles and surfaces, *Advances in Graphene Science*, Edited by Mahmood Aliofkhazraei, ISBN 978-953-51-1182-5, 2013.
2. B. Ma, C. Martín, R. Kurapati A. Bianco, Degradation-by-design: how chemical functionalization enhances the biodegradability and safety of 2D materials, *Chem. Soc. Rev.*, 49, 2020, 6224-6247.
3. X. Chen, J-H. Ahn, Biodegradable and bioabsorbable sensors based on two-dimensional materials *J. Mater. Chem. B*, 8, 2020, 1082-1092.
4. N.Y. Sreedhar, M. Sunil Kumar, K. Krishnaveni, Sensitive determination of chlorpyrifos using Ag/Cu alloy nanoparticles and graphene composite paste electrode, *Sensors and Actuators B: Chemical*, 210, 2015, 475-482.
5. J. Bao, T. Huang, Z. Wang, H. Yang, X. Geng, G. Xu, M. Samalo, M. Sakinati, D. Huo, C. Hou, 3D graphene/copper oxide nano-flowers based acetylcholinesterase biosensor for sensitive detection of organophosphate pesticides, *Sensors and Actuators B: Chemical*, 279, 2019, 95-101.
6. R. Kurapati, T.W. Groth., A.M. Raichur, Recent developments in Layer-by-Layer technique for drug delivery applications, *ACS Appl. Bio Mater.*, 2, 12, 2019, 5512-5527.
7. P. Rajapaksha, S. Cheeseman, S. Hombsch, B.J. Murdoch, S. Gangadoo, E.W. Blanch, Y. Truong, D. Cozzolino, C.F. McConville, R.J. Crawford, V.K. Truong, A. Elbourne, J. Chapman, Antibacterial Properties of Graphene Oxide-Copper Oxide Nanoparticle Nanocomposites, *ACS Appl. Bio Mater.*, 2, 12, 2019, 5687-5696.
8. D. Armstrong, R. Brown, The analysis of free radicals, lipid peroxides, antioxidant enzymes and compounds related to oxidative stress as applied to the clinical chemistry laboratory. *Adv Exp Med Biol.*, 366, 1994, 43-58.
9. B. Martinov, S. Slavov, A. Staneva, D. Dimitrov, J. Mateeva, Electric properties of new composite materials based on RGO, nanosized ZnO and Cu nanoparticles, *Journal of Physics: Conference Series*,



- 1762, 2021, 012029
10. B.L. Martinov, A.D. Staneva, T.E. Vlahov, S. Slavov, D. Dimitrov, Y.G. Marinov, G.B. Hadjichristov, Synthesis and characterization of nanosized ZnTiO<sub>3</sub> doped with reduced graphene oxide (RGO) Journal of Physics: Conference Series, 1762, 2021, 012031.
11. M. Balouiri, M. Sadiki, S.K. Ibnsouda, Methods for in vitro evaluating antimicrobial activity, A review Journal of Pharmaceutical Analysis, 6, 2, 2016, 71-79.
12. D. Kichukova, I. Spassova, A. Kostadinova, A. Staneva, D. Kovacheva, Facile Synthesized Cu-RGO and Ag-RGO Nanocomposites with Potential Biomedical Applications, Nanomaterials, 2022, 12, 2096. \_
13. A. Mai-Prochnow, M. Clauson, J. Hong, A. Murphy, Gram positive and Gram-negative bacteria differ in their sensitivity to cold plasma. Sci Rep 6, 2016, 38610, <https://doi.org/10.1038/srep38610>
14. T.D. Tavares, J.C. Antunes, J. Padrão, A.I. Ribeiro, A. Zille, M.T.P. Amorim, F. Ferreira, H.P. Felgueiras, Activity of Specialized Biomolecules against Gram-Positive and Gram-Negative Bacteria. Antibiotics, 9, 2020, 314, <https://doi.org/10.3390/antibiotics9060314>
15. S. Mathews, M. Hans, F. Mücklich, Contact killing of bacteria on copper is suppressed if bacterial-metal contact is prevented and is induced on iron by copper ions, Appl. Environ. Microbiol., 79, 8, 2013, 2605-2611.
16. M. Gupta, V.K. Mahajan, K.S. Mehta, P.S. Chauhan, Zinc Therapy in Dermatology: A Review Dermatol. Res. Pract., 2014, 709152.
17. H. Cui, Z.F. Zhang, M.J. Shi, Chemiluminescent reactions induced by gold nanoparticles, J. Phys. Chem., 2005, 109, (8) 3099–3103.
18. K. Faulkner, I. Fridovich, Luminol and lucigenin as detectors for O<sub>2</sub>, Free Radic. Biol. Med., 1993, 15, 447-451.
19. E. Pavlova, M. Lilova, V.M. Savov Study of free radical peroxidation processes in urine by enhanced chemiluminescence, Annuaire de L'universite de Sofia "St. Kliment Ohridski", Faculte de Physique, Presses Universitaires, 95, 2002, 57-69.
20. E.L. Pavlova, V.M. Savov, Chemi-luminescent in vitro estimation of the inhibitory constants of antioxidants ascorbic and uric acids in Fenton's reaction in urine, Biochemistry (Moscow), 7, 8, 2006, 861-863.
21. E.L. Pavlova, R.D. Toshkovska, Ts.E. Doncheva, I.A. Ivanova, Prooxidant and antimicrobial effects of iron and titanium oxide nanoparticles and thalicarpine, Archives of Microbiology, 202, 7, 2020, 1873-1880.
22. J.T. Hancock, R. Desikan, S.J. Neill, Role of reactive oxygen species in cell signalling pathways, Biochem. Soc. Trans., 29, 2, 2001, 345-350.
23. M. Nishikimi, N. Appaji, K. Yagi, The occurrence of superoxide anion in the reaction of reduced phenazine methosulfate and molecular oxygen, Biochem Biophys. Res. Commun., 46, 2, 1972, 849-854.